Furthermore, we use a preamplifier with a bandwidth of 250 MHz and an A/D converter with 20 GSamples/s.

The scanning unit for the equidistant 2-d scanning consists of a moving mirror for elevation scan (320 raster steps of 0.1°) and a moving platform for azimuth scan (600 raster steps of 0.1°). The field of view is 32° in vertical and 60° in horizontal direction.

2.2 Test scene

For the investigations, a measuring platform is placed at a height of 15 m, pointing at an outdoor scene. The different urban objects in the scene are buildings, streets, vehicles, parking spaces, trees, bushes, and grass. Some objects are partly occluded and the materials show various backscattering characteristics.

2.3 Scanning and data

For each orientation of the beam within the scanning pattern, the emitted signal and the received signal are recorded over the time t for the time interval $t=t_{min}$ to $t=t_{max}$. The time interval selected for the recording of the signal depends on the desired recording depth of the area (in our case up to 200m). For each discrete range value the intensity value of the pulse is stored. The entire recording of a scene can be interpreted and visualised as a discrete data cuboid I[x y t], where the measured intensity at each time t and each beam direction [x y] is stored. It has to be taken into account the recording geometry for correct interpretation of the data.

3. STRATEGY

An automatic approach for detecting laser weak pulses based on neighbourhood relation preserved in the waveform cuboid is presented in this section.

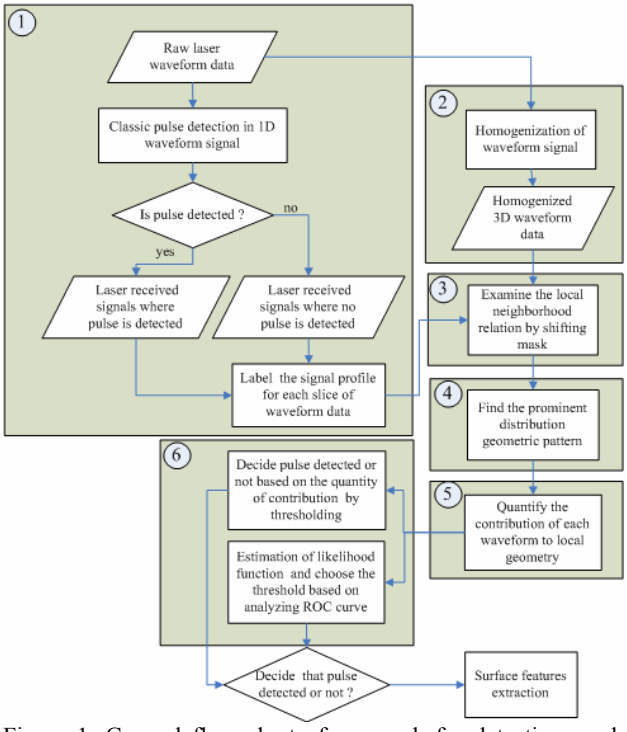

Figure 1. General flow chart of approach for detecting weak signal

The general strategy is sketched in Fig. 1. At first, a classic pulse detection method is adopted to extract the significant pulse signal backscattered from objects. Every laser ray in the waveform cuboid will be labelled as detected or undetected. On the other hand, the waveform cuboid is undergone a homogenization process. Afterwards, we generate a 1-D mask and shift it through every vertical slice of waveform cuboid to analyze the local neighbourhood relation by waveform stacking, and the prominent geometric pattern can be found. By comparing original waveforms to averaged stacked waveform the contribution of each waveform to local geometry can be assessed by a likelihood value. At last, according to this value, we can attribute a class (***'pulse', 'no pulse' or 'uncertain'***) to every original waveform by selecting thresholds in advance or by statistical inference.

3.1 Classic pulse detection method

Because of algorithmic efficiency and simplicity, it is always wise to apply the classical 1-D pulse detection methods (e.g. peak detection or correlation method) to raw waveform data firstly; high-energy reflected pulse can be detected, as displayed in Fig. 2. The rest laser rays where no pulse has been detected contain either weak reflection pulse from specific objects (e.g. window glass or roof behind the trees) or no backscattered signal at all due to inexistence of objects (sky)

Figure 2. Pulses detected by peak method, white pixels indicate detected pulses.

For pulse detection a noise dependent threshold was estimated to separate a signal pulse from background noise. Therefore the background noise was estimated and if the intensity of the waveform is above $3\,\sigma_n$ of the noise standard deviation for the duration of at least 5ns, then the waveform will be accepted.

For peak detection method, the range value of the detected pulses is determined by the maximum pulse amplitude, where the largest reflectance is expected. Another two typical surface features are roughness and reflectance which correspond to width and amplitude of waveform. Then, a Gaussian curve can be fitted to recorded waveform to get a parametric description using iterative Gauss-Newton method ((Jutzi & Stilla, 2006)). The estimated parameters for waveform features are the average time τ , standard deviation σ and maximum amplitude a .

$$w(t) = \frac{a}{\sqrt{2\pi\sigma^2}} \exp\left(-\frac{(t-\tau)^2}{2\sigma^2}\right) \qquad (1)$$

According to results of the classic pulse method, every waveform of laser beams will be labelled as detected (1) or undetected (0) and arranged in arrays corresponding to various vertical slices for further study.

The latent roots (or eigenvalues of covariance matrix $\mathbf{C}$) from the PCA define the amount of explained variance for each component, and the proportion of each variance can be derived:

$$\mathbf{C} = \mathbf{E}[\mathbf{B} \otimes \mathbf{B}] = \frac{1}{N}\mathbf{B} \cdot \mathbf{B}^*$$

$$\mathbf{V}^{-1}\mathbf{C}\mathbf{V} = \mathbf{D} \qquad (2)$$

where $\mathbf{B}$ is mean-subtracted matrix of $\mathbf{x}$, $\mathbf{D}$ is the diagonal matrix of eigenvalues of $\mathbf{C}$, $\mathbf{V}$ is matrix of eigenvectors diagonalizing the covariance matrix $\mathbf{C}$.

$$\begin{aligned} \text{roots} &= \mathbf{diagonal}(\mathbf{D}) \\ \text{propoVAR} &= \text{roots/sum(roots)} \\ &= [0.998 \quad 0.001 \quad 0] \end{aligned} \qquad (3)$$

As showed above the variance of first component has held a dominant proportion against other components according to propoVAR, the straight line is the best 1-D linear approximation to the data (Fig 5).

3.3.2 Waveform of undetected pulse

For another group of waveforms where pulse is not detected yet, we must deal with whole waveform signal instead of point cloud. Waveform stacking method is adopted to locate potential geometric pattern within the mask.

Image stacking technique is used to increase the signal to noise ratio (SNR) of weak objects in the final output image. This basic idea can be easily transformed to the concept of waveform stacking. We take the 1D signal along laser ray as the unit for waveform stacking, and try to identify prominent peak information in the stacked waveforms generated along specific slopes, which means existence of significant regular geometry such as plane. By stacking multiple waveforms on top of each other along different slopes, the weak pulse is expected to be enhanced against the random noise. The random noise will be counteracted with each other in spite of low SNR, whereas the true reflection information representing object features will be emphasised to some level, so they can be identified again.

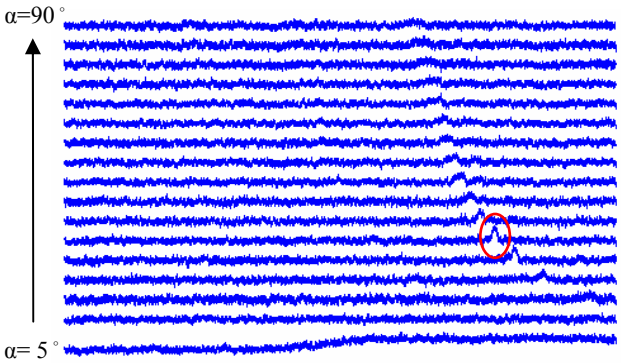

Figure 6. Waveform stacking along slope angles from $\alpha = 5^\circ$ to 90°, in steps of $\Delta\alpha = 5^\circ$ for roof area (from the slice marked by green dotted line in Fig 4a). Red ellipse marks the maximal peak information of the best stacked waveform.

Through waveform stacking, we can obtain a series of stacked waveforms corresponding to various stacking slope angles (Fig.6). When there is only one significant distribution of regular geometry like straight line, only one maximal peak signal interval of certain stacking slope angle corresponding to local geometry can be identified, and the result of waveform stacking along this slope is called best stacked waveform. If there are barely or multiple distinct peak signals, we fail to find out the regular geometric pattern in local neighbourhood due to no or ambiguity of extremum distribution, such as sky and holes and volume scatters (tree leaves).

In Fig 7 the cyan curve denotes the maximal value of stacked waveform along each slope toward stacking angle. The red curve is the smoothed version of the cyan curve. The approximation of red curve by cubic is plotted in magenta. Thus, the slope angle of best stacked waveform can be improved by locating maximum of fitting curve with "sub-pixel" accuracy. The green dotted line indicates the max value of cubic.

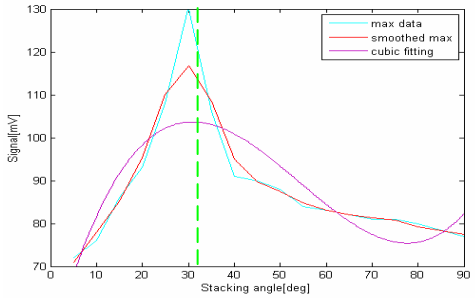

Figure 7. Maximum values of stacked waveforms vs. stacking slope angle

3.4 Find the prominent geometric pattern

After examining the local neighborhood relation for waveforms of detected and undetected pulses respectively, we have to consider them as an entirety. The local neighbourhood where both kinds of pulses coexist is examined by shifting a mask (Fig.8a). The prominent geometric pattern for a mixed set of waveforms (detected and undetected pulses) within the mask has to be identified and is to be recorded in a data list $\{\mathbf{P}_i\}$.

First we have to distinguish between three different situations encountered while shifting the mask (Fig.8b):

a) Waveform of undetected pulse almost occupies the mask, Number (Num) of $\{\mathbf{waveform\ of\ no\ pulse}\} > 9$

b) Waveform of detected pulse almost occupies the mask
Num of $\{\mathbf{waveform\ of\ pulse}\} > 9$

c) Both kinds of waveforms appear balanced
Num $\{\mathbf{waveform\ of\ pulse}\} < 9$ &Num $\{\mathbf{waveform\ of\ no\ pulse}\} < 9$

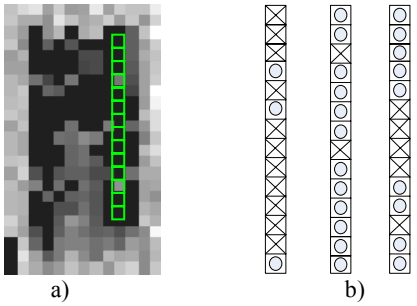

Figure 8. a) Example of mask shifted over waveform cuboid (x-y view), b) three typical situations encountered, circle indicates waveform of pulse detected, and cross indicates waveform of no pulse

perhaps due to poor local neighbourhood relation and very weak reflection.

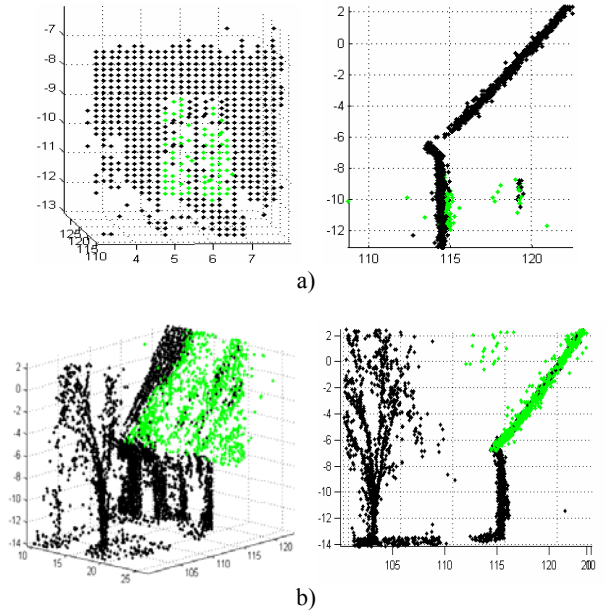

Figure 11. Results of local sections of test scene a) point cloud of window section with detected weak pulses showed in green from front and side view, b) section of roof behind the tree

After making a decision on three categories, the yellow category will be delivered to a further check based on SNR, so that we can finally obtain a result of only two classes - detected or not detected. In Fig.12 the relative histograms of correlation coefficient of two classes are depicted overlaid with each other. The Gaussian curve used to fit to the histograms can be perceived as an approximation of likelihood function for each hypothesis, few overlapping area proved separability of two classes and appropriateness of correlation coefficient as feature value.

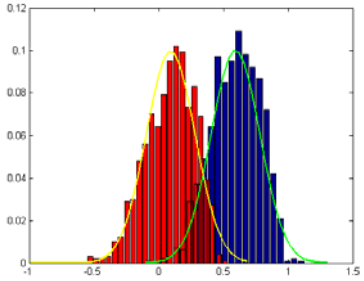

Figure 12 Overlapping relative histograms of correlation coefficients of two classes – pulse detected (blue) and not detected (red), with corresponding Gaussian fitting.

5. CONCLUSION

In this work an automatic approach for extracting weak laser pulses from full-waveform laser data has been presented. The algorithm uses waveform stacking to analyze the local neighbourhood of laser signals. Hypotheses for planes of different slopes are generated and verified. Each signal is assessed by a likelihood values with respect to accepted hypotheses. This contribution measure to local geometry is used for the subsequent operation of detection. The results on waveform data acquired from urban area show ability to detect partially occluded objects or objects with poor surface response, which can not be geometrically predicted by previous detected point cloud. In this paper only the neighbourhood relation within a vertical slice was used, Future work will focus on hypothesis generation combining neighbouring vertical slices.

References

Brenner, A.C., Zwally, H.J., Bentley, C.R., Csatho, B.M., Harding, D.J., Hofton, M.A.,Minster, J.B., Roberts, L.A., Saba, J.L., Thomas, R.H., Yi, Y., 2003. Geoscience Laser Altimeter System (GLAS) —derivation of range and range distributions from laser pulse waveform analysis for surface elevations, roughness, slope, and vegetation heights. AlgorithmTheoretical Basis Document—Version 4.1. http://www.csr.utexas.edu/glas/-pdf/Atbd_20031224.pdf (Accessed March 1, 2007).

Der, S., Redman, B., Chellappa, R., 1997. Simulation of error in optical radar measurements. Applied Optics 36 (27), pp. 6869-6874.

Hofton, M.A., Blair, J.B., 2002. Laser altimeter return pulse correlation: A method for detecting surface topographic change. Journal of Geodynamics special issue on laser altimetry 34, pp. 491-502.

Hofton, M.A., Minster, J.B., Blair, J.B., 2000. Decomposition of laser altimeter waveforms. IEEE Transactions on Geoscience and Remote Sensing 38 (4), pp. 1989–1996.

Hug, C., Ullrich, A., Grimm, A., 2004. LITEMAPPER-5600 - a waveform digitising lidar terrain and vegetation mapping system. International Archives of Photogrammetry, Remote Sensing and Spatial Information Sciences 36 (Part 8/W2), pp. 24–29.

Irish, J.L., Lillycrop, W.J., 1999. Scanning laser mapping of the coastal zone: the SHOALS system. ISPRS Journal of Photogrammetry & Remote Sensing 54 (2-3), pp. 123-129.

Jutzi, B., Stilla, U., 2003. Laser pulse analysis for reconstruction and classification of urban objects. In: Ebner, H., Heipke, C., Mayer, H., Pakzad, K. (Eds) Photogrammetric Image Analysis PIA'03. International Archives of Photogrammetry and Remote Sensing 34 (Part 3/W8), pp. 151-156.

Jutzi, B., Stilla, U., 2006. Range determination with waveform recording laser systems using a Wiener Filter. ISPRS Journal of Photogrammetry and Remote Sensing 61 (2), pp. 95-107.

Reitberger, J., Krzystek, P., Heurich, M., 2006. Full-Waveform analysis of small footprint airborne laser scanning data in the Bavarian forest national park for tree species classification. In: Koukal, T., Schneider, W. (Eds) 3D Remote Sensing in Forestry, pp. 218-227.

Söderman, U., Persson, Å., Töpel, J., Ahlberg, S., 2005. On analysis and visualization of full-waveform airborne laser scanner data. Laser Radar Technology and Applications X. In: Kamerman, W. (Ed) SPIE Proceedings Vol. 5791, pp. 184-192.

Wagner, W., Ullrich, A., Melzer, T., Briese, C., Kraus, K., 2004. From single-pulse to full-waveform airborne laser scanners: Potential and practical challenges. In: Altan, M.O. (Ed) International Archives of Photogrammetry and Remote Sensing 35 (Part B3), pp. 201-206.